Global Positioning System over Fiber for Buoyant Cable Antennas

Adil M. Karim, Stephen J. Stafford, and R. Benjamin Baker

*B*uoyant cable antennas (BCAs) are long, towed antennas used by submarines to receive RF signals. Deployed while the submarine is operating at depth, the cable is managed so that the internal antenna element or elements are positioned near the ocean surface. The received signal is sent to the submarine for processing over a transmission line within the cable. In this article, we examine the design of a fiber-optic signal transport link for a BCA that receives signals from the Global Positioning System (GPS). This signal and reception method is of significant interest because the resulting GPS solution can be fused with the submarine's inertial navigation system to improve overall navigation accuracy without requiring the ship to come to periscope depth.

INTRODUCTION

The evolution of network-centric warfare requires that submarines have the ability to send and receive RF signals. Submarines have generally been forced to come to periscope depth and expose a mast antenna or deploy a buoy to use the electromagnetic spectrum. These actions increase detectability and the risk of collision. However, the development of buoyant cable antennas (BCAs) has enabled a new mode of operation where a submarine can remain at depth and still receive RF signals. This cable contains the active antenna element or elements as well as the transmission line that carries the received signal to the submarine for processing. The trailing length of cable is managed using an inboard deployment system and passes through a seal that maintains watertight integrity for the ship. The focus of this article is on the design of a fiber-optic network for transport of Global Positioning System (GPS) signals collected from multiple antenna elements within the BCA, as shown in Fig. 1. The signals are transported from the receiving antennas to a shipboard location through a process known as antenna remoting.

The diameter of the cable is constrained so as to reduce observability and mechanical risk. A typical BCA has an outer diameter of 0.65 in., including the
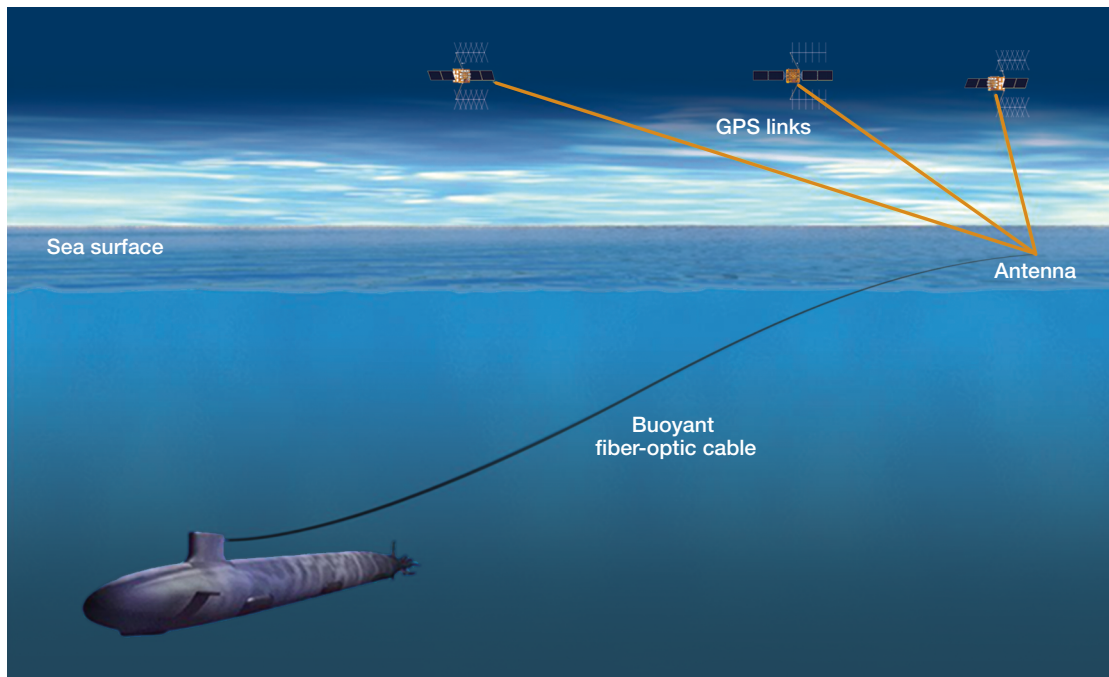
Figure 1. Submarine with deployed BCA for reception of GPS signals.

outer jacket and any internal structure. The maximum length of any rigid section is 1.0 in., for compatibility with inboard BCA handling equipment. These two factors severely limit the size of the antenna elements and supporting electronics. Performance is further limited by the ocean surface, which introduces attenuation for submerged or partially submerged antennas. In addition, the conductivity of seawater has a strong impact on the actual antenna pattern.

The resulting disadvantaged nature of the antenna and the long length of the cable mean that transport in the electrical domain is not feasible at higher frequencies. Even with the use of electronic amplifiers, the substantial propagation loss increases the noise figure of the system. Noise figure is a term that measures the degradation in signal-to-noise ratio (SNR) caused by a component or system. This increase in noise figure means that the receiver sensitivity is reduced and that many signals of interest will not be processed successfully. We show that for cables exceeding a certain length, the use of fiber optics for remoting of received GPS signals offers a distinct performance advantage.

GPS OVERVIEW

Historically, submarines have used low-frequency Long Range Navigation (LORAN) signals to determine their location and speed. However, this system has been replaced in recent years by the NAVSTAR GPS. This is a Global Navigation Satellite System (GNSS) that provides worldwide radio coverage from a constellation of satellites. The satellite constellation consists of at least 24 satellites in medium Earth orbit that transmit a variety of direct sequence spread spectrum (DSSS) signal ranging codes, as shown in Fig. 2.

A network of terrestrial control stations provides the satellites with accurate time and position information. This information is encoded in the signals transmitted by the GPS satellites, enabling users on the ground to extract the propagation time from the satellite to the
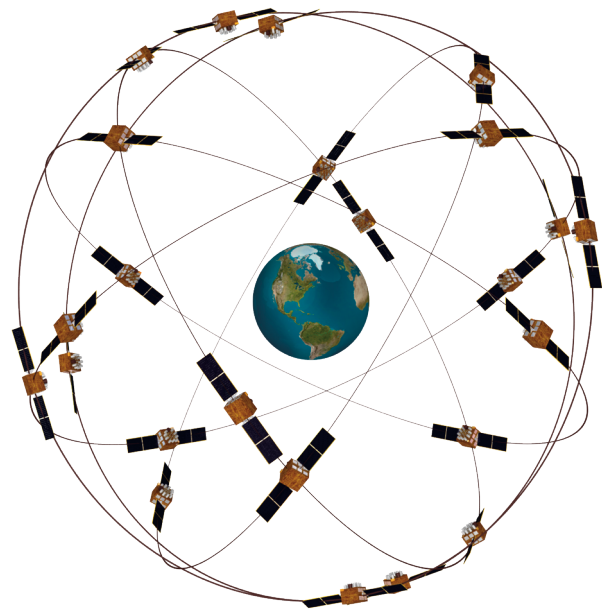

Figure 2. GPS satellite constellation in medium Earth orbit.

receiving antenna by demodulating the received signal. This propagation time can be used to estimate a pseudo-range, an estimate of the distance from the antenna to an individual satellite. The pseudo-range, ρ_i, to the ith satellite is given by

$$\rho_i = |P - P_i| + cT,\qquad (1)$$

where P is the user's position, P_i is the ith satellite's position, c is the speed of light, and T is the error contribution from the receiver's clock. Equation 1 would be used to determine the user's position once sufficient pseudo-range information has been obtained.

The GPS system transmits several DSSS ranging signals, the most important of which are the civilian Coarse Acquisition (C/A) signal centered at the L1 frequency (1575.42 MHz) and the two military Precision P(Y) signals centered at the L1 and L2 (1227.60 MHz) frequencies. The P refers to a precision signal with greater accuracy than the C/A signal, and P(Y) refers to the encrypted version of this signal. For the purposes of this article, the principal difference between the civilian and military signals is their bandwidth. The C/A signal has a bandwidth of 2.046 MHz, and the P(Y) signal has a bandwidth of 20.46 MHz. In addition to the ranging signal, each satellite transmits a navigation message including clock corrections and almanac and ephemeris information. The clock corrections, almanac information, and ephemeris information are required to synchronize the satellite atomic clocks with terrestrial receiver clocks. The almanac message contains coarse orbit information for all satellites in the constellation and can be used to determine which satellites are within the receiver's field of view. This reduces the receiver search time. The ephemeris message contains precise orbit information for the individual satellite. This orbital information is required to minimize errors resulting from minor variations in the satellite's orbit. The ephemeris data are valid for only a few hours and must be updated periodically. A position is calculated through trilateration, which requires pseudo-ranges from at least four satellites in a nondegenerate geometry to solve for the user's four unknowns: latitude, longitude, altitude, and receiver clock error. Pseudo-range measurements from additional satellites improve the geometry and allow integrity monitoring.[1]

GPS SIGNAL RECEPTION IN BCAs

The principal difficulty with GPS signal reception over the

BCA is attenuation along the RF signal path. This includes propagation through the atmosphere, potential propagation through seawater, antenna gain that is limited by the BCA geometry, and, finally, propagation along the BCA transmission line to the GPS receiver. The GPS signal level for antennas at or slightly above the ocean surface is approximately –130 dBm, where dBm refers to the power ratio in decibels relative to 1 mW. Over the sampled bandwidth of the C/A signal (2.046 MHz), the integrated thermal noise is approximately –111 dBm. For an antenna gain of 0 dBi, this means that the SNR at the antenna is –19 dB. The term dBi refers to the gain of the antenna under consideration (in decibels) compared to that of an isotropic antenna, which radiates uniformly in all directions. Although this number seems low, a significant amount of processing gain (43 dB) can be achieved by despreading the DSSS signal. For a target sensitivity of –140 dBm (providing 10 dB of link margin), the SNR at the antenna is –29 dB. This 10 dB of link margin can be used to compensate for propagation losses or accommodate antenna detuning caused by the ocean surface. A typical GPS receiver requires an SNR of 10 dB after despreading, which is equivalent to an SNR of –33 dB prior to despreading. Comparing the SNR at the antenna with the required SNR, we see that the antenna and receive link can only degrade the SNR by 4 dB before the received signal becomes unusable. The penalty caused to the SNR by a component or subsystem is known as the noise figure, expressed in decibels. On the basis of this calculation, the GPS BCA receive path must have a noise figure of less than 4 dB. The numbers provided here are approximate values, but they do indicate that the BCA receive link must have a low noise figure nearly equal to that of conventional GPS receive links, which need to operate over only a short length of cable.

Receiving GPS signals over a BCA is further complicated by the operating environment, shown in Fig. 3. The antenna is presented with two obstacles: seawater washover and cable roll that can align the antennas downward. Even mild antenna washover rapidly attenu-
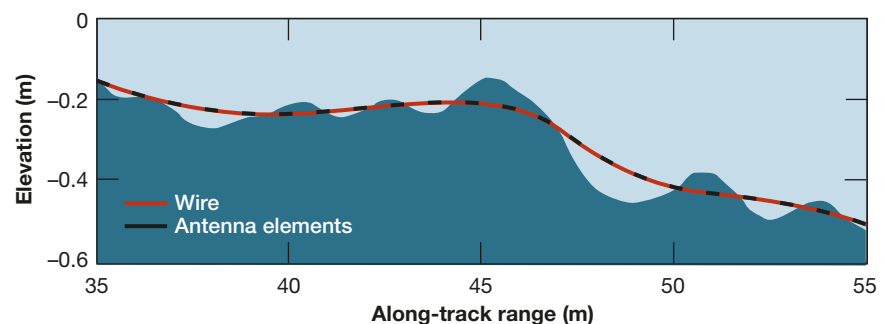

Figure 3. BCA floating on ocean surface. Some antenna elements are submerged or partially submerged.

ates GPS signals—the attenuation of RF at L1 in seawater is more than 1000 dB/m.[2] These impediments can be overcome through redundancy. The proposed system consists of 12 GPS antennas separated by 8–10 ft each along the cable. Each antenna is capable of independently receiving GPS signals, and this approach prevents a single wave from washing over the entire array. In addition, the antennas are aligned at offset angles of 120° with respect to each other along the length of the cable. This mitigates the antenna performance degradation caused by uncertain roll of the cable and eliminates the possibility of all antenna elements being oriented downward. This rotation pattern repeats for each of the four sets of three antennas. The antennas used during system development were tuned to a 2-MHz bandwidth to collect the C/A signal. We anticipate that future versions of this antenna will have a wider bandwidth to support collection of the P(Y) signal.

In-water testing of the BCA indicates that a single antenna can successfully collect brief segments of GPS signals between waves as the antennas go in and out of the water. For sea states 2–3, the typical segment duration was on the order of 100 ms, and the duration of the GPS dropouts was of the same magnitude. While above water, the carrier-to-noise density ratio was 30–35 dB-Hz, which is sufficient to provide a high probability of signal detection. The signal segments are frequent enough that closed-loop delay-locked loops can support clock and data recovery despite the intermittent signal, which allows the successful extraction of pseudo-range values. However, obtaining a phase lock and estimating carrier phase from a single element under these conditions is not possible. Inboard processing is discussed in more detail in the *GPS Signal Processing* section.

FIBER OPTICS FOR ANTENNA REMOTING

Figure 4 is a block diagram of a fiber-optic antenna remoting link for use in BCAs. In this case, because GPS is the primary signal of interest, only the receive function is considered. The primary pieces of inboard
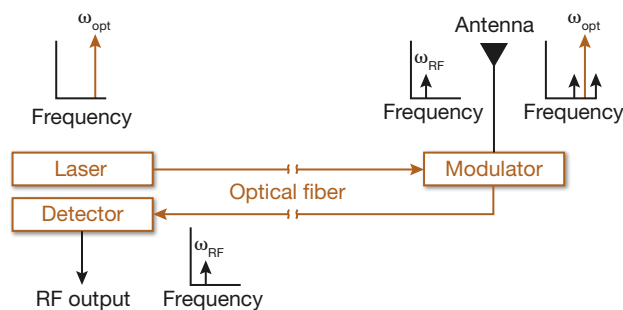

Figure 4. Block diagram of fiber-optic link for antenna remoting.

equipment are a laser and photodetector. The laser is a semiconductor-based component that generates an optical carrier at a frequency of approximately 193 THz, indicated by ω_{opt} in Fig. 4. This unmodulated optical carrier passes over a length of fiber-optic cable with nearly no attenuation because of the highly transparent nature of the glass inside the cable. At some distance away from the laser and inside the BCA, an electro-optic modulator is used to up-convert the RF signal at ω_{RF} from the antenna onto the 193-THz optical carrier. The modulated carrier is sent back to the photodetector on a fiber-optic cable. The photodetector is a square-law device and recovers the original RF signal of interest. This particular architecture is highly attractive because the laser and detector are inside the submarine, with only the modulator outboard. Arranging the components in this fashion rather than using an outboard laser reduces the number of active components in the cable and relaxes outboard thermal design constraints.

In some ways, a fiber-optic link is similar to traditional RF mixing for free space propagation, because the signal of interest is being up-converted to take advantage of superior propagation characteristics at the higher frequency. The down-conversion from optical to RF takes place at the photodetector. A fiber-optic link can be treated like a long RF amplifier, in that it has an RF input and an RF output and can be characterized by its gain, noise figure, and distortion characteristics. Compared with conventional electronic links operating over coaxial cable, fiber-optic links can provide significant advantages in bandwidth, propagation loss, and weight, as well as immunity to crosstalk and electromagnetic interference.

Bandwidth and propagation loss can be considered together, because the signal loss is a function of frequency. In this area, fiber optics offers superior performance relative to coaxial cables. Consider the Times Microwave LMR-LW400, a flexible, lightweight, low-loss coaxial cable commonly used for GPS remoting applications that is nominally compatible with BCA mechanical requirements.[3] The propagation loss of LMR-LW400 at the principal GPS frequency (1.6 GHz) is 50 dB/1000 ft. By comparison, the optical loss in a single-mode fiber is 0.06 dB/1000 ft. The actual RF signal loss in optical fiber is 2 × 0.06 dB = 0.12 dB/1000 ft, because RF power is proportional to the square of photocurrent, and photocurrent is proportional to optical power. For a 2000-ft BCA (a typical length), the signal loss in this coaxial cable would be 100 dB, whereas the signal loss in optical fiber would be only 0.2 dB. This highlights the significant advantage of fiber optics in antenna remoting over extended distances.

To accurately compare optical link performance to electrical link performance, the efficiency of the electrical–optical-electrical conversion process must be

considered along with the fiber-optic propagation loss. The inefficiency of this process limits fiber-optic link gain, which sets a lower limit on link noise figure. The fiber-optic link noise figure can be further degraded by laser relative intensity noise and shot noise from the photodetection process. Assume that a low-noise electrical amplifier with a gain of 60 dB and a noise figure of 2 dB is available for use between the antenna and the coaxial transmission line or between the antenna and the electro-optic modulator. Figure 5 shows the link noise figure as a function of distance for frequencies of 1.6 GHz in LMR-LW400 and through a fiber-optic link. The calculated noise figure of the fiber-optic link is based on COTS components and includes conversion efficiency, propagation loss, and the additive noise factors discussed above. The same comparison is made at 10 and 20 GHz. Although these frequencies are not used for GPS, they are of interest for future BCA applications and are included here to illustrate performance at higher frequencies and the scalability of a fiber-optic BCA. For the GPS signal, the fiber-optic link has a lower noise figure than the coaxial link for distances greater than 800 ft. The crossover distances for 10 and 20 GHz are 300 and 200 ft, respectively. For a distance of 2000 ft, the crossover frequency at which the fiber-optic link has a lower noise figure is approximately 300 MHz. The noise figures of the fiber-optic links are slightly greater than 2 dB as a consequence of inefficiencies in the electrical–optical–electrical conversion

process, photodetector shot noise, and relative intensity noise from the laser. Additional background on analog fiber-optic link performance and design methods is available in Refs. 4–6.

In theory, it is possible to use multiple electrical amplifiers to reduce the noise figure of the electrical link. However, this approach has severe disadvantages. The additional active components increase complexity and power consumption while reducing reliability. From an RF perspective, increasing the amplifier count reduces the dynamic range and input power damage threshold. Down-conversion of the received GPS signal to a lower intermediate frequency is another possible option, but this option still requires a high degree of outboard component complexity, including active components.

Weight is an important factor because the BCA must be nearly neutrally buoyant for the trailing antenna to reside at or above the surface during operation. The weight per unit length of a fiber-optic cable is typically much lower than that of a coaxial cable, particularly when both cables are inside the protective BCA jacket. The coaxial cable considered above, Times Microwave LMR-LW400, has a weight of 50 lb per 1000 ft of cable. In contrast, a standard single-mode fiber with a protective coating has a weight of 1 lb per 1000 ft. For a 2000-ft BCA, the total weight savings are approximately 98 lb without any loss in capability. Another view would be that for the same weight allocation, additional fibers can be installed to 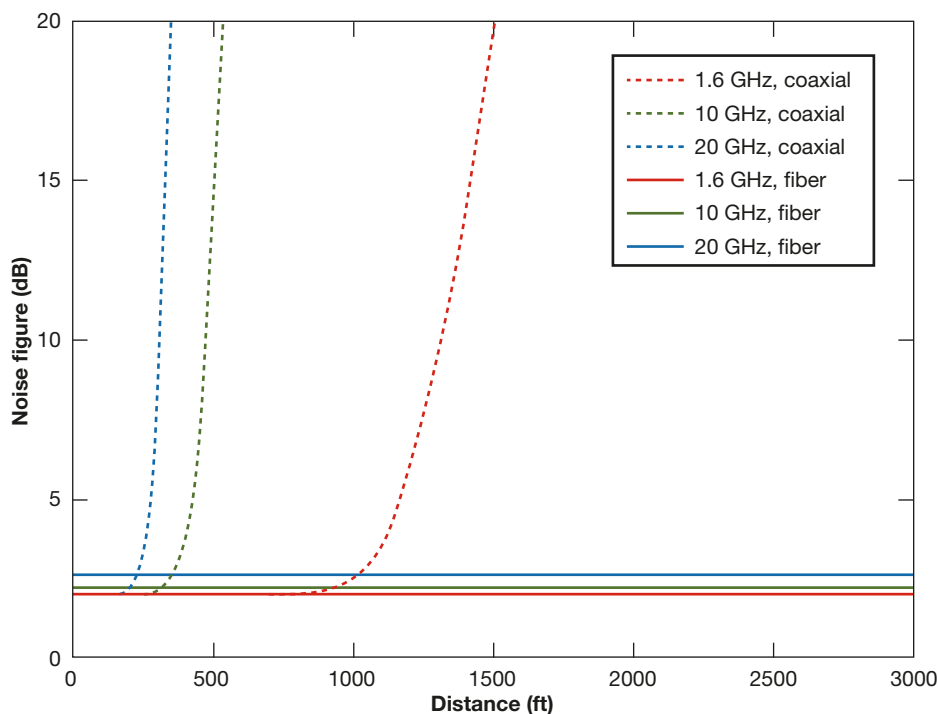improve system scalability or provide additional functionality. For example, the additional fibers could support future system expansion or provide redundancy in case of a fiber break, antenna failure, or electronics failure. This is impossible with a BCA containing a single conventional coaxial cable.

Because sea states and wave conditions vary, it is difficult to guarantee that a single antenna element in a BCA will be at, rather than below, the surface. Thus it is highly desirable to use multiple antenna elements and process the received signals from each of them.[7] When remoting multiple antennas in a constrained space such as a BCA, electromagnetic interference and crosstalk can be significant in conductive cables. Because a
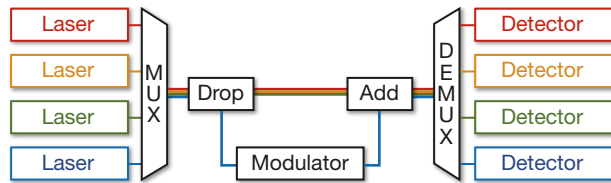

Figure 5. Noise figure comparison between optical fiber and coaxial cable at frequencies of 1.6, 10, and 20 GHz.

Figure 6. Wavelength division multiplexing using passive optical components. DEMUX, demultiplexer; MUX, multiplexer.

fiber-optic cable is all-dielectric, it is immune to electromagnetic interference and to crosstalk from adjacent fibers. Furthermore, a single fiber-optic line can be used to carry numerous RF signals at identical or different frequencies using multiple optical carriers in a technique known as wavelength-division multiplexing.[8] In this architecture, passive optical elements with low insertion loss are used to multiplex, filter, and demultiplex modulated optical carriers with negligible levels of crosstalk between the various signals. An example is shown in Fig. 6. Four lasers at different wavelengths are combined using a 4 × 1 multiplexer so that the output can be carried on a single optical fiber. At an intermediate point in the system, one wavelength is dropped from the stream using a narrowband optical filter. This wavelength is then modulated with an RF signal and added back to the stream using a second optical filter. The four-wavelength stream, with a single modulated wavelength, is then demultiplexed, with each wavelength going to a different photodetector. The crosstalk between the electrical outputs from each photodetector is generally better than –60 dB and can be better than –80 dB. These values are more than sufficient for successful electronic demultiplexing of the received signal. The passive optical filters described here are key elements in enabling a BCA system architecture that is robust and scalable.

BCA SYSTEM DESIGN

On the basis of the noise figure analysis described in the preceding section, as well as the other advantages of optical networks, a fiber-optic backbone is the proper design choice for higher-frequency (>300 MHz) BCA systems. Although the emphasis of this design is the reception of GPS signals, an additional goal is to provide a backbone that can scale to higher frequencies of interest. This backbone can consist of one fiber or multiple fibers. Consider the case where the BCA contains 12 individual antenna elements. These elements could be remoted by two fibers using

12 wavelengths, as shown in Fig. 7. One fiber would be used to transmit 12 unmodulated optical carriers, while 12 modulated optical carriers would return on the second fiber. However, the fiber plant itself would be a single point of failure in this architecture, since damage to the fiber or an optical filter could disable the entire system. Redundancy can be provided by using multiple fibers. Using 12 fiber pairs would provide full independence between antenna elements but would have a high degree of mechanical complexity. An intermediate number of fiber pairs, such as four, can be used to provide some redundancy without the challenges of a fully independent remoting architecture. This preferred option is illustrated in Fig. 8. Note that the use of 12 separate antenna elements also provides some degree of redundancy, because any one antenna is capable of receiving a GPS signal. Overall availability would be reduced if fewer than 12 antenna elements were accessible, but limited functionality would still be available. Additional details on the availability of individual elements and the overall system concept are given elsewhere.[7]

An additional constraint on the number of fibers is imposed by the requirement to use fiber-optic terminations between sections to support modular replacement and future expansion. Commercially available terminations that meet form-factor requirements support a maximum of 12 fibers. Four wavelengths are used for each of the four fiber pairs, with the appropriate drop and add filters at each antenna element. These wavelengths are indicated by the colors red, orange, green, and blue in Fig. 8. The wavelengths are staggered so that each module is identical and could be replaced by a universal spare. Using three wavelengths for active remoting on each of the four fiber pairs leaves one wavelength per fiber pair unused. The additional wavelength can be used for future expansions by simply connecting an additional antenna module. This expansion capability can support additional GPS antenna modules or a different type of antenna module.

For this antenna remoting architecture, multiple optical carriers are generated inboard using semiconductor lasers. The outputs of semiconductor lasers are horizontally polarized. The optical modulators used in the outboard portion of the BCA respond efficiently only when used with horizontally polarized light. Ordi-
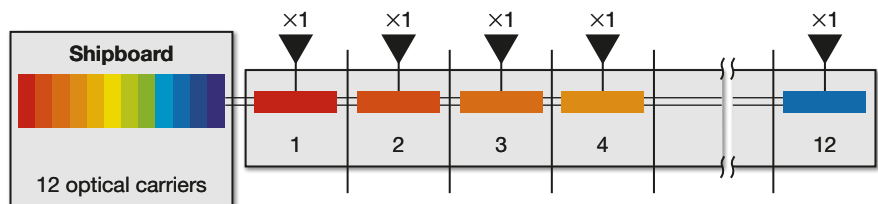

Figure 7. BCA with a single fiber pair. The fiber plant is a single point of failure.
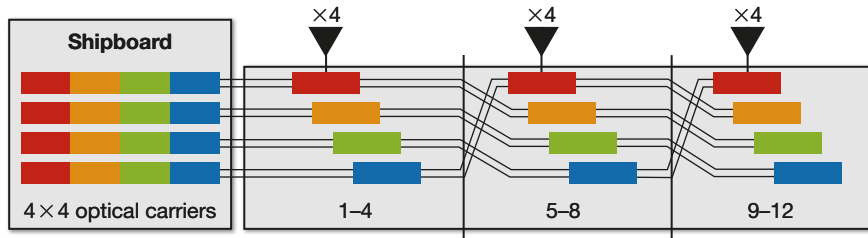
Figure 8. BCA with wavelength-division multiplexing and extra fiber pairs for redundancy.

narily, the horizontal polarization could be maintained over the length of the BCA by using polarization-maintaining fiber. However, the requirement to use optical terminations between sections of the outboard cable eliminates this possibility. There are no commercially available multiple-fiber terminations that maintain polarization across the termination, although there are terminations available that support 12 standard fibers. The cost of polarization-maintaining fiber is also much greater than that of standard fiber. As a result, an alternative method of delivering horizontally polarized light to the modulator over standard fiber was required. In a standard fiber, the polarization state varies based on temperature, mechanical stress, and other environmental conditions. A concept developed for this project was to use a dual-polarization optical carrier consisting of two closely spaced, orthogonally polarized optical wavelengths. The two wavelengths are closely spaced so that they see the same polarization rotations as they propagate through standard fiber. An in-fiber polarizer is used prior to the modulator that scatters vertically polarized light and passes horizontally polarized light. Half of the source light is lost, but a horizontally polarized component of constant magnitude is always delivered to the modulator. This architecture is illustrated in Fig. 9 for two example scenarios. Even though the amount of polarization rotation in the standard fiber varies, the two components remain orthogonal. The final composition of the horizontal
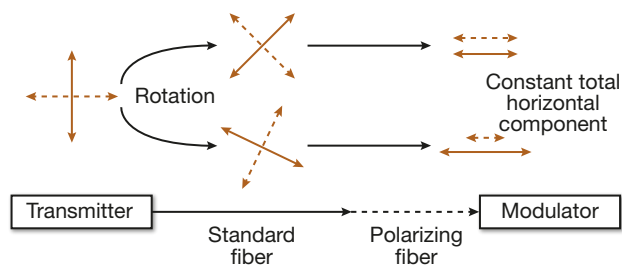

Figure 9. Polarization rotation of transmitted carrier components and selection of horizontal component by polarizing fiber. Even though the amount of rotation varies in the two cases shown, a total horizontal component of constant magnitude is delivered to the modulator.

component delivered to the modulator changes, but its magnitude is constant. The remaining passive components in the optical path are not polarization sensitive, so no additional polarization management is required. When the two modulated components are incident on the photodiode, the RF output signals from each individual wavelength are summed. For a given input signal, this ensures a constant output signal level over varying cable conditions.

The frequency spacing between the two wavelengths used to generate the composite carrier is an interesting point for discussion. If the two source wavelengths were very closely spaced (<50 GHz apart), the possibility of coherent interference would exist because of beating between the two sets of modulation sidebands. This effect might only be significant at higher frequencies (>10 GHz) but is still worth considering because the fiber plant should support future growth. If the two wavelengths were too far apart (>400 GHz), the polarization variation would not be constant across this span and there would be no guarantee that a horizontally polarized component would be delivered to the in-fiber polarizer or the modulator. An intermediate spacing of 200 GHz was chosen to meet performance requirements and simplify component selection. At this spacing, there are no concerns about interference effects at the photodiode.

For the initial engineering demonstration, a BCA system containing three antenna nodes was designed and assembled. This small-scale demonstration was intended as a proof-of-concept for the larger 12-node system. The number of nodes and optical carriers used was reduced relative to the 12-node design, but the basic functionality and architecture are identical. System details are provided here for the three-node engineering demonstration model. The composite optical carriers are designated in Fig. 10 by $\lambda 1\pm$, $\lambda 2\pm$, and $\lambda 3\pm$. The actual system uses two fiber pairs that each carry three composite carriers. For clarity, Fig. 10 shows only a single fiber pair from Fig. 9. The remaining fiber pairs are identical (except for the staggered wavelength plan) and include redundant inboard hardware. From an optical perspective, the BCA consists of four independent two-fiber networks, each carrying four wavelengths. Each two-fiber network can be extended by using the fourth reserved wavelength or simply adding more wavelengths. The composite carriers are combined on a single fiber using an optical multiplexer. An optical amplifier (not shown) is used to boost the optical carrier levels prior to entering the outboard portion of the
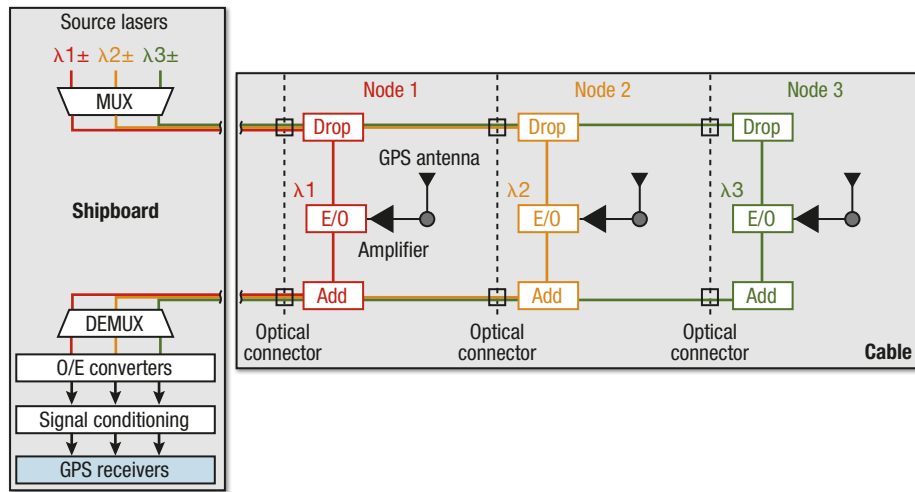
Figure 10. Block diagram of BCA optical network. A single fiber pair is shown for clarity. The actual network consists of four such fiber pairs with a staggered wavelength plan. E/O, electrical-to-optical conversion; O/E, optical-to-electrical conversion.

BCA. An inboard patch cable is used to connect the amplifier output to the transmission line. The transmission line passes through a fiber-optic rotary joint and the ship's handling gear before exiting the submarine. Electrical-to-optical conversion takes place at the block labeled E/O, and optical-to-electrical conversion takes place at the block labeled O/E.

A detailed illustration of the antenna node is shown in Fig. 11. At the first antenna node, the first carrier (orange) is dropped for modulation. A standard thin-film optical filter is used to drop the carrier of interest while allowing the other two carriers to pass through. Both the drop and the through paths have low insertion loss of less than 0.7 dB each. The polarization state of the carrier has changed after passing through the fiber but still consists of two orthogonal components. A polarizing fiber passes the horizontal component of the carrier and scatters the vertical component. The carrier is then modulated using a lithium niobate Mach–Zehnder modulator (the E/O modulator in Fig. 11). This is a common modulator type for RF and microwave applications. The modulator used in this project is reflective, meaning that input (unmodulated) and output (modulated) fibers are on the same side of the device. A bias controller is used to maintain an optimal operating point for the electro-optic modulator. This controller generates a low-frequency pilot tone and monitors an internal modulator photodiode

as part of a feedback control loop. The GPS signal received by the antenna is amplified before reaching the optical modulator. The purpose of this amplifier chain is to set the noise figure of the overall link by compensating for the losses and the additive noise of the fiber-optic portion. A second filter is used to return the modulated carrier to the multiple-wavelength stream. The components are spaced along the cable in individual housings to meet the diameter and rigid-length constraints.

The modulated carriers return to the submarine on the second fiber, as shown in Fig. 10, and pass through the handling gear. A second optical amplifier with variable gain is used to compensate for variable loss levels in the fiber-optic rotary joint as the deployed cable length is increased or decreased. The carriers are then demultiplexed, with each composite carrier being routed to a photodetector. The electrical output from each photodetector is the sum of the two modulated carrier components, as described above. This approach eliminates fading and guarantees a constant signal level over varying polarization conditions. The electrical outputs from the photodetectors (O/E in Fig. 10), which consist of the received GPS signals plus gain and noise from the link, are passed to inboard processing units for signal conditioning and demodulation. This process repeats at the other two nodes at different wavelengths.

FIBER-OPTIC LINK PERFORMANCE

The noise figure is the key figure of merit in evaluating GPS link performance. For the GPS signal to be suc-
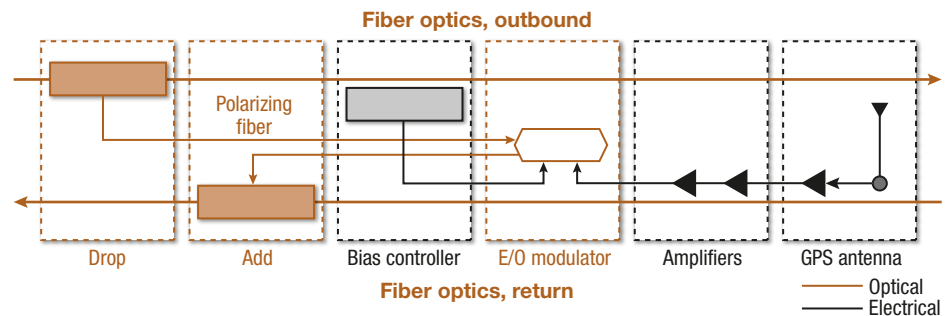

Figure 11. Detailed illustration of antenna node architecture.

cessfully demodulated, the noise figure of the electrically pre-amplified fiber-optic link is specified to be less than 3.0 dB, providing 1 dB of margin against the 4-dB figure mentioned earlier. The noise figure for the optical portion of the link is determined by laser noise, optical amplifier noise, modulator efficiency, and the received photocurrent level.[4] Recent advances in component design and novel link architectures have resulted in fiber-optic links with noise figures of less than 10.0 dB without electrical pre-amplification.[5,6,9] However, the constraints on rigid length in the BCA severely limit modulator efficiency. As a result, the BCA fiber-optic link has a gain of –36 dB and a noise figure of 42 dB at 1.6 GHz. This is comparable to the performance level that would be expected using a standard commercial fiber-optic link, but in a much more challenging geometry.

Considering the fiber-optic link noise figure of 42 dB, a significant amount of electrical pre-amplification is required to reduce the overall link noise figure to less than 3 dB. Because GPS adoption has been so widespread, there are a number of high-performance, low-noise amplifiers to choose from. Many parts have noise figures of less than 1.0 dB. For this application, a three-stage amplifier with a total gain of 50 dB and a noise figure of 1.5 dB was assembled using commercially available components. The gain stages are separated physically as shown in Fig. 11, both to prevent oscillation and to meet BCA rigid-length constraints. The first stage is integrated directly with the antenna to limit front-end losses.

Cascade analysis can be used to calculate the overall link noise figure. Because of the large amount of low-noise gain prior to electro-optic modulation, the combined link has a gain of 14 dB and a noise figure of 1.9 dB. The gain and noise figure for the electrical preamplifiers, the fiber optics, and the combined link are summarized in Table 1. This link budget includes realistic component values and cable loss between components.

The calculated link noise figure of 1.9 dB is lower than the 4 dB requirement estimated above (see the *GPS Signal Reception in BCAs* section) and provides some additional margin against unexpected losses and component degradation. This low noise figure is a necessary but not sufficient condition for successful processing of the GPS signal.

Table 1. Cascaded noise figure for GPS over fiber link

Subsystem	Gain (dB)	Noise figure (dB)
Electrical	50.0	1.5
Optical	–36.0	42.0
Total	14.0	1.9

GPS SIGNAL PROCESSING

The GPS ranging codes are overlaid with a BPSK (binary phase shift keying) navigation message at a data rate of 50 bits/s. This message contains necessary information for accurate positioning (see the *GPS Overview* section) and must be decoded from each satellite individually. Each message frame contains 1500 bits and has a duration of 30 s. The clock correction and ephemeris information are included in each message frame and repeat every 30 s. The almanac information is distributed over 25 message frames. The demodulation process is complicated by the fact that the received GPS signal levels from the BCA rise and fall with a period of approximately 100 ms due to wave action. During the strong signal portions, the GPS message can be demodulated. A reconstruction algorithm can be used to fuse the handful of bits that are demodulated from each segment. The combining algorithm leverages the 30-s repetition of the message and the forward error correction within the message to combine the demodulated bits across the antennas. A voting scheme uses the probability of bit error to favor bits from strong signals. Hardware-in-the-loop tests in the Chesapeake Bay indicate that this approach is capable of decoding the message in an acceptable amount of time.

This system differs from conventional GPS systems in that the signals are received on an array of 12 antennas. The pseudo-range model from Eq. 1 is generalized for the multi-antenna system to include an antenna index j:

$$\rho_i = |P_j - P_i| + cT + cT_j, \qquad (2)$$

where ρ_i is the range to the ith satellite, P_j is the location of the jth antenna, P_i is the position of satellite i, T is the receiver clock error, and T_j is the propagation delay from the jth antenna to the receiver. The antenna-specific delay T_j includes the propagation through the BCA to the receiver on the submarine. This delay can be directly characterized during assembly by using a network analyzer or can be calculated using the cable length and group delay of individual components. Likewise, the offset of each antenna relative to the first antenna can be predicted. This offset can be estimated through knowledge of the relative distance between the antennas along the BCA and the BCA's orientation, which is known from the inertial navigation system aboard the submarine. The correction for the offset can then be applied to the measurements from antennas 2 through 12. With knowledge of the relative propagation delays and position offsets, Kalman filtering and other signal processing techniques can be used to extract a composite GPS solution from the (up to) 12 independently received GPS signals.

ACCURACY OF THE GPS MEASUREMENTS

Reconstructing the GPS navigation message from intermittently received signals is the primary challenge for this BCA system. Once the signals have been received, stitched together, and demodulated, the noise sources and overall accuracy for each received signal can be analyzed in the same manner used in more conventional GPS systems. The pseudo-range measurements described in Eq. 2 have several sources of noise, including receiver measurement noise, satellite positioning and timing errors, atmospheric delays, and multipath errors. The pseudo-range noise maps directly into positioning error through the dilution-of-precision multiplier. The dilution-of-precision multiplier converts pseudo-range uncertainty to position uncertainty and is between 1 and 5 for most applications.

Receiver noise is a random measurement error and a function of the carrier-to-noise ratio C/N_0. This thermal noise–dominated error is well approximated by Eq. 3:

$$\sigma_{RCVR} = c\tau \sqrt{\frac{B}{(2C/N_0)}\left(1 + \frac{2}{T_{CO}C/N_0}\right)} \text{ (meters), (3)}$$

where σ_{RCVR} is the receiver noise error, τ is the chipping period of the DSSS signal, B is the tracking loop bandwidth, T_{CO} is the integration time, and C/N_0 is the signal strength in linear units. This expression applies to delay lock loop discriminators with an early–late separation of half a chip. The C/A chipping period is roughly 1 μs. The tracking loop bandwidth is on the order of

1 Hz and T_{CO} is typically 10 ms. For characteristic signal strengths, the receiver noise is approximately 5–10 m.

The 1-σ satellite position error is on the order of 1 m for fresh ephemeris information.[10] However, the ephemeris is optimized over a 4-h window. Outside that window, the ephemeris quality degrades. This is relevant for disadvantaged antennas such as the BCA because the GPS pseudo-range measurement could become available before the GPS message is fully decoded. If this occurs, ephemeris error becomes a primary driver of noise. For example, ephemeris information that is 6 h old has a mean error of roughly 75 m.

There are two predominant sources of atmospheric error: the ionosphere and the troposphere.[11] These two regions introduce propagation delays that affect GPS accuracy. The ionosphere is a dispersive medium that extends from 50 to 1000 km above Earth's surface. Ionospheric delay is a function of the total electron content along the path of the RF signal, and it varies with time of day. Because the ionospheric delay is a well-characterized function of frequency, dual frequency receivers using L1 and L2 can measure and remove the ionospheric error. However, the current version of the BCA is limited to signal reception at L1 only. The unmitigated ionospheric error is typically between 1 and 10 m, depending on the time of day and the phase of the solar cycle. The troposphere is the lowest layer of the atmosphere and extends from the surface of Earth to an altitude of approximately 16 km.[11] Tropospheric delays produce errors of 2–3 m for satellites above an elevation angle of 20°. The most significant tropospheric
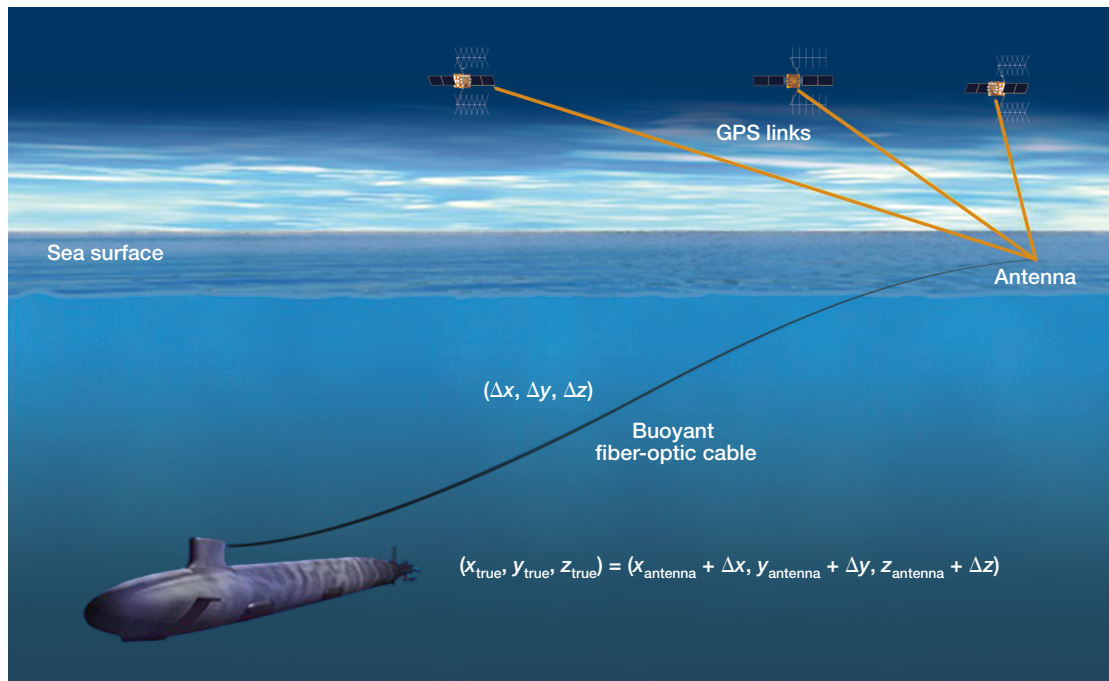

Figure 12. Correction for offset of GPS antenna position.

errors can be eliminated by an elevation mask that discards signals from satellites at lower elevation angles. The tropospheric error for higher-elevation satellites can be modeled and reduced to roughly 10 cm.

For many GPS receivers, multipath interference is also an area of concern. However, the GPS BCA operates in a broad ocean area and is not significantly affected by multipath interference. Like tropospheric error, multipath interference can be avoided by masking signals from satellites at low elevation angles.

GPS NAVIGATION

Signals received at different antennas will have a position offset that is described by the antenna index in Eq. 2. A correction term can be applied to refer each measurement to the position of the first antenna. This offset can be estimated through knowledge of the distance between the antennas and the orientation of the BCA. The 12 individual antennas are separated by 8 to 10 ft, as shown in Fig. 3. The orientation of the BCA can be estimated using the submarine's inertial measurement unit. A correction is then applied to the measurements from antennas 2 through 12. This can be accomplished by correcting the individual pseudo-ranges for offsets between antennas or by correcting the calculated position solutions for each antenna. Signal processing techniques for reconstruction and correction of the received signals are currently being evaluated.

The GPS receiver generates a position solution for the antenna, not for a point on the submarine. This makes it necessary to estimate the offset between the GPS receiver and the first antenna, since the precise path of the GPS transmission line is unknown. Traditional techniques use catenary models to determine the offset between antenna and receiver, but these have large uncertainties in their accuracy. A number of techniques, including fiber-optic position sensing, are under consideration for providing a corrected GPS solution that accounts for the separation between the antenna and the submarine as well as for individual antenna positions. This concept is illustrated in Fig. 12, where true coordinates (x_{true}, y_{true}, z_{true}) are determined by taking reported coordinates ($x_{antenna}$, $y_{antenna}$, $z_{antenna}$) and adding an offset (Δx, Δy, Δz) that corresponds to the cable path. The calculated positions are then integrated in a Kalman filter, along with input from the shipboard inertial navigation system and other navigation sensors, to generate a navigation solution.[12]

CONCLUSIONS

BCAs enable submarines to receive RF signals without requiring the ship to come to periscope depth. The ability to receive GPS signals over a BCA is especially valuable because these signals can be used to determine a navigation solution without exposing a mast or deploying a buoy. The use of fiber optics enables low-noise antenna remoting over extended distances, which is particularly important over the long length of the BCA for a sensitive signal like GPS. Compared with coaxial remoting, fiber optics has significant advantages in bandwidth, scalability, propagation loss, weight, and immunity to electromagnetic interference. With the BCA deployed for extended intervals, GPS becomes a valuable navigation aid and possibly even a navigation source. Future work in this area will include development of position- sensing techniques to accurately determine the offset between the GPS antenna and the receiver. Other areas of interest for BCA research include the development of phased arrays and photonic transmit modules for two-way communication capability at speed and depth. An engineering model of the system described here underwent successful field testing in summer 2011 and development efforts are continuing.

REFERENCES

[1]Parkinson, B. W., and Spillker Jr., J. J., *Global Positioning System: Theory and Applications Vols. 1 and 2*, American Institute of Aeronautics, Washington, DC (1996).

[2]Jackson, J. D., *Classical Electrodynamics*, John Wiley and Sons, New York (1998).

[3]Times Microwave Systems, *LMR-400 Datasheet*, http://www.timesmicrowave.com/products/lmr/downloads/22-25.pdf (accessed 26 Jan 2011).

[4]Cox, C. H., *Analog Optic Links: Theory and Practice*, Cambridge University Press, New York (2004).

[5]Karim, A., and Devenport, J., "High Dynamic Range Microwave Photonic Links for RF Signal Transport and RF-IF Conversion," *IEEE J. Lightwave Technol.* **26**(15), 2718–2724 (2008).

[6]Clark, T., O'Connor, S., and Dennis, M., "A Phase-Modulation I/Q-Demodulation Microwave-to-Digital Photonic Link," *IEEE Trans. Microwave Theory Techniq.* **58**(11), 3039–3058 (2010).

[7]Thompson, G., Widmer, H., Rice, K., Ball, R., and Sweeney, J., "Buoyant Cable Antenna Technology for Enhancing Submarine Communications at Speed and Depth," *Johns Hopkins APL Tech. Dig.* **20**(3), 285–296 (1999).

[8]Ramaswami, R., and Sivarajan, K., *Optical Networks: A Practical Perspective*, Morgan Kaufman Publishers, San Francisco (1998).

[9]Ackerman, E. I., Burns, W. K., Betts, G. E., Chen, J. X., Prince, J. L., et al., "RF-Over-Fiber Links with Very Low Noise Figure," *IEEE J. Lightwave Technol.* **26**(15), 2441–2448 (2008).

[10]GPS Operations Center, *GPS Documentation*, https://gps.afspc.af.mil/gpsoc/gpsdocumentation.aspx (accessed 2 Feb 2011).

[11]Misra, P. E., and Enge, P., *Global Positioning System: Signals, Measurements and Performance*, 2nd Ed., Ganga-Jamuna Press, Lincoln, MA, p. 157176 (2006).

[12]Grewal, M., Weill, L., and Andrews, A., *Global Positioning Systems, Inertial Navigation and Integration,* John Wiley & Sons, Hoboken, NJ, pp. 382–424 (2007).

The Authors

Adil M. Karim

Stephen J.
Stafford

R. Benjamin
Baker

Adil M. Karim is a member of the Senior Professional Staff in the Electro-Optic and Infrared Systems Group in APL's Air and Missile Defense Department. His technical interests include fiber optics for antenna remoting, microwave photonics, optical component design, and fiber-optic sensing. He was the fiber optics technical area lead for the project described in this article and is involved in a number of other fiber-optics programs at APL. **Stephen J. Stafford** is a member of the Senior Professional Staff in the Force Projection Department. Since joining the GNSS and SATRACK Systems Group in 2005, his work has included the development of signal-processing techniques for radio navigation. His work on this project included development of algorithms for recovery of GPS message segments received from multiple antennas. **R. Benjamin Baker** is a member of the Senior Professional Staff and a Section Supervisor in the Force Projection Department. His technical interests include high-frequency monolithic microwave integrated circuit (MMIC) design, high-efficiency microwave power amplifiers, and microelectronic assemblies. His work on this project included design of microelectronic assemblies for use in the GPS receive path. For further information on the work reported here, contact Adil Karim. His e-mail address is adil.karim@jhuapl.edu.

The *Johns Hopkins APL Technical Digest* can be accessed electronically at **www.jhuapl.edu/techdigest**.